



Mapping woody vegetation cover across Australia's arid rangelands: Utilising a machine-learning classification and low-cost Remotely Piloted Aircraft System



J. Barnetson*, S. Phinn, P. Scarth

University of Queensland, School of Earth and Environment Sciences, Remote Sensing Research Centre, Saint Lucia, Brisbane, QLD, Australia

ARTICLE INFO

Keywords:
Remotely Piloted Aircraft System (RPAS)
Sentinel2
Planet Dove
Ortho-mosaic
Drone
Landsat

ABSTRACT

Knowledge of the extent and degree of wooded vegetation cover in the arid parts of Australia is essential for land-holders and management agencies. The balance between wooded and ground-cover vegetation is important to livestock production and landscape health. Adequate mapping of changes in wooded vegetation cover allows the assessment of its expansion and contraction as input for improved management of production and conservation. The aim of this study was to develop a method to accurately map the extent and degree of wooded tree and shrub cover across an area of arid rangeland in central Australia. Its open and sparse distribution throughout the landscape and its adaptation to an arid environment present challenges to obtaining both representative field measurements and scale appropriate remotely sensed imagery. Recent advancements and access to high spatial resolution satellite imagery provide opportunities for improved mapping. The rapid development of Remotely Piloted Aircraft Systems (RPAS) or drones also provides further opportunities to improve the accuracy of field measurements used in the classification of wooded vegetation. An optimised machine-learning classification was developed using high resolution Planet Dove cube-sat and Sentinel2 imagery and compared to medium resolution Landsat8 imagery. An efficient method of collecting plot scale (ha) wooded vegetation cover estimates for the training and assessment of the satellite image classification was also developed using the RPAS. It was comparable to other field based measurements. The results of the classifications showed a moderate degree of accuracy in distinguishing wooded cover from non-wooded cover, highest with the Planet Dove imagery. An improved accuracy in distinguishing between wooded cover classes was also seen in the Sentinel2 classification. The mapping and subsequent monitoring of wooded vegetation in these landscapes has been shown to be improved with higher resolution satellite imagery.

1. Introduction

Wooded or woody vegetation are terms used interchangeably that refer to lignified tree and shrub vegetation. Woody thickening is the term that refers to increases in trees and shrubs in woodlands and is associated with the absence or reduction of burning (Fensham, 2008), often the result of overgrazing (Noble, 1998). As Witt et al. (2009) state; changes in the density of wooded vegetation have the potential to reduce livestock productivity and adversely affect natural ecosystem processes. Wooded tree and shrub cover balances with that of grassland pasture for livestock production are needed throughout the arid rangelands of Australia. Empirical evidence of wooded vegetation thickening occurring in the arid rangelands, spanning several decades is limited to a number of published studies including Witt et al. (2009) analyses of 50-years of aerial photography for an area of arid wooded

vegetation in western Queensland, Sinclair (2005) study in Koonamore Reserve 1926–2002 in South Australia and Gardiner et al. (1998) appraisal of woody shrub encroachment in western New South Wales. A gap in the knowledge of the extent and density of wooded vegetation cover, including its possible expansion or contraction, exists across other parts of arid Australia.

Aerial photography and other high resolution space borne remotely sensed imagery, generally less than 1 m in spatial resolution, has been traditionally used to map wooded vegetation in these landscapes (Bowman et al., 2008; Wang et al., 2015; Witt et al., 2009). In their development of a remotely sensed image scaling procedure in arid Australia, Ludwig et al. (2006) suggest that a pixel resolution should be equal to or smaller than the size of the focal scale, in this case the canopy of the individual trees and shrubs of low and sparse arid wooded vegetation. High spatial resolution imagery provides such a

* Corresponding author.

E-mail addresses: j.barnetson@uq.edu.au (J. Barnetson), s.phinn@uq.edu.au (S. Phinn), p.scarth@uq.edu.au (P. Scarth).

resolution. As Fisher et al. (2017) suggests, a number of challenges exist in using higher resolution imagery from both air and space borne platforms to map large areas of wooded vegetation, namely cost and consistent geometric and radiometric properties through space and time. The use of medium and low resolution imagery, generally greater than 1 m in spatial resolution, is more common in woodlands and forests throughout Australia (Lu et al., 2003; Gill et al., 2009, 2017; Fisher et al., 2016; Danaher et al., 2010; Armston et al., 2009). A number of these studies reported that mapping *Acacia* dominated arid to semi-arid woodlands was problematic with these sensors. Gill et al. (2017) reported that they were not mapped due to either being classed as not woody or having low Foliage Projected Cover (FPC). The latter likely the result of the morphological and physiological adaption of vegetation to an arid climate. Armston et al. (2009) in his prediction and validation of FPC from Landsat imagery across Queensland reported that in *Acacia aneura* dominated woodlands, inaccuracies in FPC estimates were likely also the result of low photosynthetic vegetation and their adaptations to drought. Gill et al. (2017) concluded that higher spatial resolution imagery may help in these landscapes. Spectral un-mixing methods have been used to quantify the proportions of arid wooded and non-wooded vegetation in medium spatial resolution imagery. Wang et al. (2015) conducted a Linear Spectral Mixture Analysis (LSMA) to derive woody cover from Landsat imagery in the same arid landscape of this study. Although they reported that accurate woody cover can be estimated from dry period Landsat imagery by LSMA, they concluded that a more convenient method of measuring woody cover using high spatial resolution imagery should be conducted to ensure the validity of estimates of woody cover derived from Landsat imagery.

Recent advancements in space born technologies include the launch and operation of the European Space Agency Sentinel constellation of satellites, of particular benefit to this study are the medium to high spatial resolution Sentinel2A and 2B satellites. They provide freely available 10 m multi-spectral imagery every 5–10 days on average over the study area. In addition to the Sentinel2 imagery the commercial cube-sat company Planet have launched a constellation of over 120 small scale satellites, providing high resolution (3–5 m) visible to near infra-red imagery on a similar repeat visit schedule to that of Sentinel2 across the study area. The imagery is available under a research and development licence.

Further challenges exist in acquiring field based observations and measurements of arid wooded vegetation characteristics for training and assessment of remotely sensed classifications and products. The two nationally accepted methods in Australia include the star transect point intercept method of Muir et al. (2011) and the grid transect point intercept method of White et al. (2012). Both are proven rigorous methods of measuring both woody and ground cover vegetation, however a number of limitations in arid wooded vegetation have been observed. In the experiences of the author in establishing several hundred field sites using the star transect method as part of the Northern Territory Governments rangeland monitoring program (DENR, 2017), under sampling of the wooded component in sparse arid shrub-lands was observed. This may be due to the number of transects and their associated canopy intercept estimates not adequately sampling both within a canopy as well as between them. The grid pattern of a further seven transects as used by White et al. (2012), was tested in this study to overcome under-sampling of both sparse individual canopies and sparsely spaced canopies, however this was resource intensive and limiting in its practical application. A solution exists in the rapid development of Remotely Piloted Aircraft Systems (RPAS) or drones. Low cost RPAS can be used to capture high resolution (< 2 cm) aerial photography in a rapid and resource efficient manner. This can be further used to classify wooded vegetation cover extent at the field plot scale, so as to inform satellite based wooded vegetation cover classifications.

The objective of this study was to further develop existing remote sensing techniques to accurately map wooded vegetation across an area

of arid rangelands in Australia, utilising recent advances in high resolution earth observation satellites and a Remotely Piloted Aircraft System. The RPAS was used in the first stage of the study involving the collection of training and testing wooded cover field data. Each hectare field site was flown following an extended dry period to maximise the distinction between evergreen wooded vegetation and that of senescent non-wooded ground-cover vegetation. An ortho-mosaic of each sites individual RPAS aerial photos was produced to a resolution of 1.6 cm. Each ortho-mosaic was then classified into wooded and non-wooded vegetation using an object based segmentation process similar to that of the method developed by Staben et al. (2016) to derive FPC from high resolution aerial photography. Using the conceptual scaling procedure of Ludwig et al. (2006), a scaling-up process was undertaken to develop a proportional wooded cover field data set from each classified ortho-mosaic to each satellite image pixel resolution. This was then used in the training and testing of a machine learning classification of each satellite image product. An optimisation process was carried out to select the most appropriate machine learning classification algorithm and its associated input parameters. Classification image products and their associated accuracies were produced and compared.

The study developed an accurate and efficient method of collecting plot scale wooded vegetation cover estimates for both training and assessment of a satellite image classification. The classifications demonstrated the practical application of both Planet Dove and Sentinel2 imagery. The Planet Dove classification showed a higher degree of accuracy in distinguishing wooded cover from that of non-wooded cover. The Sentinel2 classification illustrated an improved ability to distinguish differences between wooded cover classes. The result of the Sentinel2 imagery having a greater radiometric range. In comparisons of both Planet Dove and Sentinel2 to that of the medium resolution Landsat8 classification, overall classification accuracy was demonstrated to increase, suggesting that higher spatial scale imagery was better suited to this type of mapping task. Improved mapping and subsequent monitoring of wooded cover change in arid landscapes is possible. On-going improvements should focus on further assessing the RPAS method of accurately sampling wooded vegetation at the field site and further collection of RPAS field data to improve the accuracy of future high resolution imagery classifications.

2. Study area and context

2.1. Arid rangelands

The Australian arid rangelands, illustrated in Fig. 1, are described by Peel et al. (2007) and the National Land and Water Resources Audit (2001) as landscapes with low, episodic rainfall and impoverished soils. As a result the vegetation is a mixture of arid adapted or xeromorphic shrub and grass lands. The study area, within these arid lands (see Fig. 1), is a largely intact natural landscape of approximately 3 million km². Less than 5% has been cleared for agriculture, horticulture or urbanisation (ABARES, 2016) and mining, tourism and livestock production are the main economic activities. Rangeland grazing for beef and sheep production is the most extensive land use, encompassing approximately 50% of the area (ABARES, 2016).

2.1.1. Pilot area

The pilot study area illustrated in Fig. 1 is located on the Old Man Plain Research Station (OMPRS) on Owen Springs Reserve, managed by the Northern Territory Department of Primary Industries (NTDPI), provided an accessible and representative landscape. Located approximately 30 km south west of the outback town of Alice Springs, the research station established in 2009 is now managed in a conservative rotational grazing strategy. Prior to 2009 the property was in a degraded state having been intensively grazed for beef production, as one of the earliest pastoral leases in the Northern Territory.

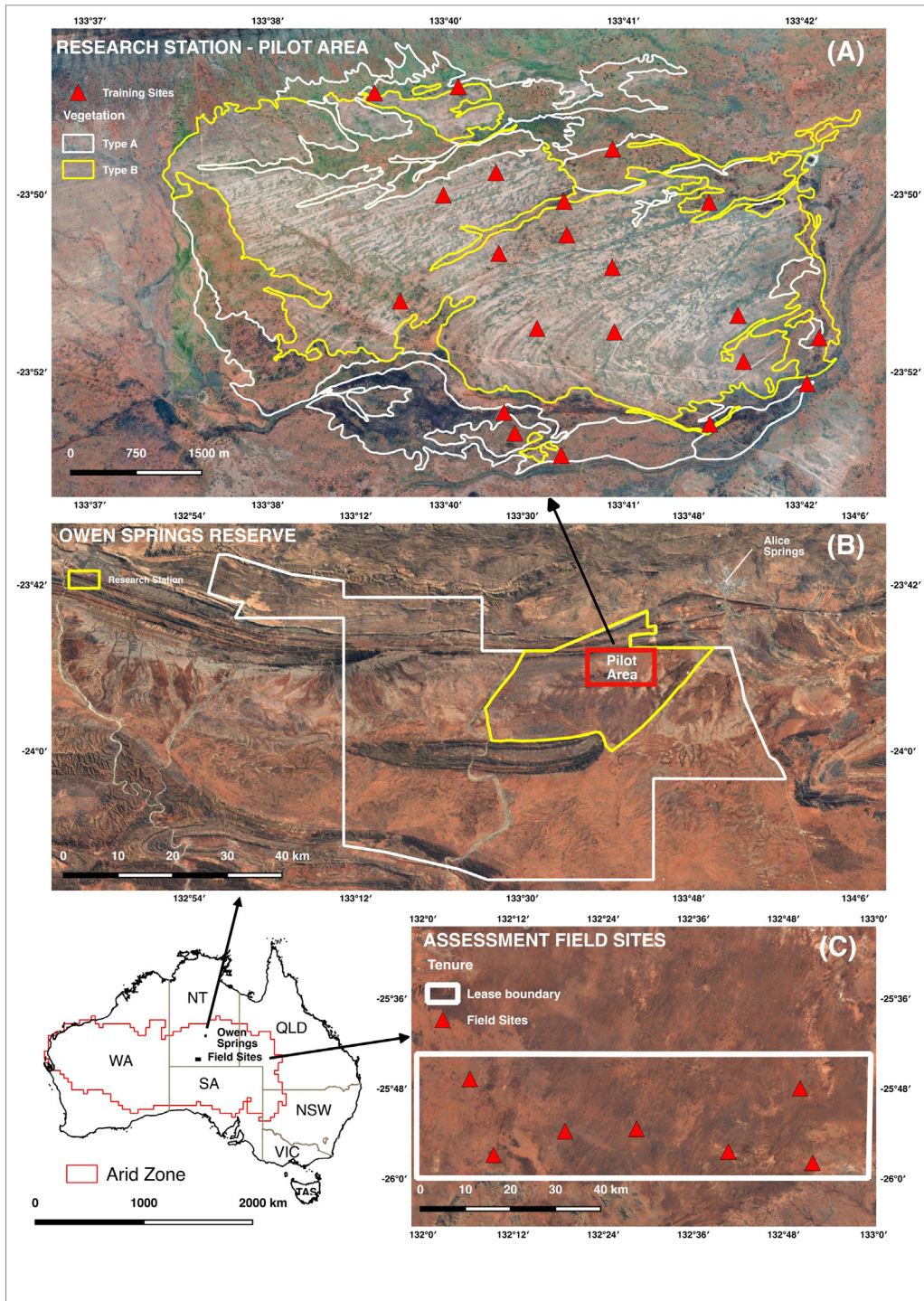


Fig. 1. Locations of (A) pilot study area with RPAS training sites and vegetation/land-form types consisting of type A – *Acacia aneura* (Mulga) in drainage areas and type B – *A. aneura* (Witchetty Bush) on calcareous plains, (B) Owen Springs Reserve and the Old Man Plain Research Station and (C) assessment field sites on neighbouring property.

2.2. Wooded vegetation stratification

The landscapes of the OMPRS are a mixture of open plains, drainage systems, mountain ranges and associated hills and foot slopes. The vegetation is dominated by *Acacia* shrub species and native and introduced annual and perennial tussock and hummock grasses. Vegetation and land-form mapping developed by Lennartz and Whitehouse (2002) was used to further stratify an area of approximately 50 km² as a mixture of *Acacia* shrub species at varying densities

and consisting of two main landforms. The first, calcareous plains, are the dominant land form and are sparsely covered with low wooded shrubs, the second, in contrast, are the drainage systems that are densely covered with taller wooded shrubs as illustrated in Fig. 1.

2.2.1. Wooded vegetation characteristics

The main wooded shrubs are Mulga (*Acacia aneura*) and Witchetty Bush (*Acacia kempeana*). *A. aneura* growing to an average height of 5–10 m and *A. kempeana* 2–5 m. Average canopy widths for both species



Fig. 2. Examples of arid woody plant adaptations. Plate (A) illustrates the open nature of the canopy and vertical arrangement of leaf structures, plate (B) shows the sparse and clumping individual shrubs, plate (C) shows small needle like leaf adaptations and plate (D) illustrates the open and low habit of the vegetation.

range from 50 cm to 1 m in shallow soils up to 2–4 m in deeper soils. The ratio of wooded non-photosynthetic plant and stem material to photosynthetic material changes in both species, as an adaptation to an arid climate, that is illustrated in Fig. 2. Plate (A) shows the open and vertically orientated leaves of the canopy that reduces solar exposure and moisture loss. Plate (B) illustrates the sparse and clumping nature of individual plants, the result of limited soil moisture and nutrients. Plate (C) shows the grey and needle like leaves of both species, *A. aneura* typically 1–13 mm wide and *A. kempeana* 4–25 mm wide. These are thick leaf-like stem structures called phyllodes, these reduce moisture loss through reduced transpiration and as a result reduced photosynthesis. Plate (D) lastly shows the open and low stunted form of a wooded arid shrub, also the result of limited moisture and nutrient availability. Wang et al. (2010) and Zandler et al. (2015) explain that such adaptations present challenges to their detection and mapping with remote sensing.

3. Materials and methods

The methodology used in this study is summarised in Fig. 3 and consists of three main stages. The first involves the development of a RPAS based vegetation cover sampling which is then used in the second stage of training a suitable machine-learning classification to map wooded vegetation cover across the study area. The third and final stage involves the assessment of the accuracy of the classification.

3.1. Wooded cover sampling

3.1.1. Remotely Piloted Aircraft System (RPAS)

A low cost drone, referred to as a Remotely Piloted Aircraft System (RPAS) by the Australian Civil Aviation Safety Authority (CASA), was utilised to capture high spatial resolution (2 cm) geo-referenced visible colour imagery. A DJI Mavic pro hobby level aircraft was used to

capture individual nadir-pointing RGB images in an 8-bit jpeg format. A total of 22 approximately 1 hectare field sites, randomly placed across the two stratified wooded vegetation types, illustrated in Fig. 1, were flown. A campaign on October 23, 2017 between 10 am and 2 pm, following a six month period with < 10 mm rainfall recorded at the nearby Alice Springs Airport recorded by the Australian Bureau of Meteorology Weather Recording Station to highlight the distinction between evergreen woody vegetation and dry senescent non-woody vegetation and thereby test the methods ability to accurately map woody vegetation under optimal conditions. An additional seven field sites illustrated in Fig. 1 were flown under similar climatic, landscape and vegetation conditions to the first campaign on May 15, 2018 between 10 am and 4 pm, on a pastoral property approximately 250 km to the south of the pilot area. These sites were collected with coincidental field measures of wooded cover and used for an assessment of the RPAS classification. Approximately 200 individual images per site were obtained with 80% side, forward and aft overlap. A circular polarising filter was used on the 12 mega-pixel aircraft RGB camera. Each site was flown in a series of parallel flight paths at a height of 50 m above ground level.

3.1.2. RPAS image processing

The OpenDroneMap (ODM) software program was used to process each field sites individual images into a 8-bit ortho-mosaic geo-referenced geo-tiff image. ODM is a free open-source UAV photogrammetry software platform that is run in a virtualisation docker container environment. The highest resolution ortho-mosaic options were selected in the Web Open Drone Map (WebODM) graphical user interface of ODM and processing took on average one to two hours on a high performance laptop computer per site.

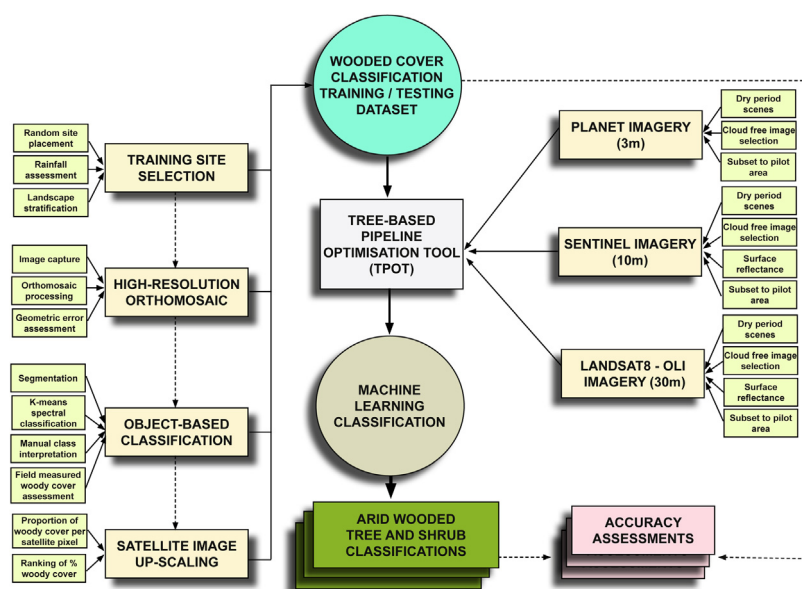


Fig. 3. Flow diagram of wooded classification methodology.

3.2. Satellite data and pre-processing

Three remotely sensed satellite products were used to classify wooded vegetation across the pilot study area. These are subsequently discussed and summarised in Table 1.

3.2.1. Planet Dove

Beginning with the highest spatial resolution of the three products, the Planet Dove constellation is made up of multiple launches of groups of individual satellites, each a small $10\text{ cm} \times 10\text{ cm} \times 30\text{ cm}$ Cube-sat (PlanetLabs, 2016). One hundred and twenty individual sun and non-sun synchronous Cube-sats orbit the earth providing daily coverage. The Planet Dove surface reflectance data was acquired for the same day or as close to the RPAS field site, and that were cloud free, were downloaded from the Planet website under their education and research access program. Each 16-bit ortho-rectified image has three spectral bands in the visible and one in the NIR spectrum, each with a three metre pixel resolution. Sensor radiance is processed to top of atmosphere reflectance and then atmospherically corrected to bottom of atmosphere reflectance from a series of MODIS satellite derived atmospheric models (PlanetLabs, 2018). No Bidirectional Reflectance Distribution Function (BRDF) corrections were applied to the imagery. Given the flat nature of the terrain over the immediate pilot area and low ($< 2\text{ m}$) height of the vegetation, BRDF effects were assumed to be insignificant.

3.2.2. Sentinel2

The Sentinel2 multi-spectral sensor is the next high spatial resolution sensor used in the study. The European Space Agency (ESA) sentinel constellation consists of a number of active and passive sensors,

Table 1
Remotely sensed satellite data details.

	Planet Dove	Sentinel2	Lsat8(OLI)
Pixel size (m)	3	10	30
No. of bands	4	4	7
BRDF corrections	x	✓	✓
Offset (days)	1	8	-24
Scene	Orthoscene	t53klp	p102 r76
Date	24-10-2017	31-10-2017	25-09-2017
Time (ACST)	10:04 am	10:47 am	10:31 am

the multi-spectral Sentinel2 A and B satellites sample across 13 spectral bands. The first four bands in the visible and NIR spectrum at a resolution of 10 m were used in the study to provide adequate spatial and spectral resolution. A surface reflectance model developed by Flood (2017) was applied to the imagery. Cloud free image acquisition was again as close as possible to the RPAS campaign.

3.2.3. Landsat8 OLI

Landsat8 – Operational Land Imager (OLI), a medium spatial resolution sensor, is the last sensor used in the classification. The first seven spectral bands at a spatial resolution of 30 m were utilised. Flood et al. (2013) and Flood (2014) atmospheric, topographic and BRDF radiometric calibrations were applied to the L1 Landsat8 data to derive surface reflectance imagery. Suitable cloud free imagery closest to the RPAS campaign was 24 days prior.

3.3. Wooded cover classification

The next section details the individual stages of the wooded cover classification including the methods used to develop a training data set, the steps used to train and develop a machine-learning based wooded cover classification of the three satellite image products and the steps undertaken to assess the accuracy of the classification.

3.3.1. Training data set

The classification was trained using each individual RPAS ortho-mosaic aerial photography, classified into wooded and non-wooded cover. Utilising the python language scikit-image modules 'quick-shift' image segmentation algorithm developed by Vedaldi et al. (2008), vegetation cover in each ortho-mosaic was first classified into individual image objects. Next, the average pixel values of each of the three ortho-mosaic bands for each cover object was calculated and an unsupervised clustering algorithm used to group objects into similar spectral classes. A mini-batch k-means clustering algorithm, developed by Sculley (2010) and made available in the machine learning sklearn python language module, classified each object into a number of spectral classes. Next, a manual assignment was carried out in a GIS of the spectral classes. Each class was overlaid on the ortho-mosaic and a simple wooded/non-wooded classification assigned to that class based on the easily distinguishable classes evident in the high resolution 3 cm RPAS imagery.

The next stage involved the use of the Ludwig et al. (2006) principle

Table 2

Training site sample pixels per cover class.

Class	Planet Dove	Sentinel2	Landsat8
Non-wooded	10,006	491	18
Class 1 (low)	5577	686	56
Class 2 (medium)	1329	215	23
Class 3 (high)	558	78	11
Totals	17,470	1470	108

of scaling-up from the ortho-mosaic classification of wooded cover to Satellite Wooded Cover (S_{WC}). This involved the calculation of the proportion of ortho-mosaic wooded pixels in each of the three overlapping coarser scale satellite image pixels. This was to produce a measure of the density of wooded cover in each satellite image pixel across each field site. All 22 field sites were amalgamated into one S_{WC} training data-set per satellite image sensor. Pixels in each data-set were then categorised as either non-wooded, low, medium and high wooded cover classes using the natural breaks classification technique of [Jenks \(1967\)](#) to determine class break points. [Table 2](#) details the number of training pixels in each class per satellite sensor.

3.3.2. Machine-learning classification

A machine-learning approach to classifying each of the three satellites used was carried out using the sklearn python language module. The S_{WC} training set was used in the development of each satellite sensor machine learning classifier model. The Tree-based Pipeline Optimisation Tool (TPOT) developed by [Olson et al. \(2016\)](#) was used to determine the most suitable machine-learning classifier and its optimal input parameter values by way of comparing and assessing two chosen classifiers and a range of input values. The Random Forest (RF) and Gradient Boost (GB) classifiers were selected as candidate models based on their performance in previous studies ([Rodriguez-Galiano et al., 2012](#); [Lawrence et al., 2004](#)). The default TPOT 10-fold cross-validation procedure using a 75/25 split was employed to train and test 10,000 model configurations to find the most suitable model and its associated parameters. Each selected optimised model was then applied to its associated satellite image.

3.3.3. Accuracy assessments

Two types of assessment were completed, the first assessment of each satellite models prediction of wooded cover and the second a validation of each sites wooded cover ortho-mosaic classification with that of field measured wooded cover.

3.3.4. Simulated accuracy assessment

An assessment of each S_{WC} model was first conducted. A Monte-Carlo simulation, similar to the re-sampling technique evaluated by [Lyons et al. \(2018\)](#), was run for several thousand iterations with each iteration randomly selecting training and testing data. In each iteration the S_{WC} model developed from the TPOT optimisation was fitted with 75% of the data and a prediction tested with the remaining 25%. The omission error, whereby the classification omits a true value, and the commission error, as a false indication of a true value, of each wooded and non-wooded cover class prediction was calculated and stored. The distribution of the overall average accuracy and error from all of the iterations was then used to illustrate the stability of the machine-learning model and the variability of each satellite sensors ability to map wooded cover. A confusion matrix of the mean commission and omission error of each S_{WC} class was calculated from all of the individual simulation assessments as was the mean overall classification accuracy and mean overall omission and commission errors from every simulation. The Kappa statistic of [Cohen \(1960\)](#) from each confusion matrix was also calculated as an overall measure of the performance of each classification.

3.3.5. Field data validation

A validation of a number of field site wooded cover ortho-mosaic classifications was next carried out to assess the accuracy of the classification to map wooded cover. The assessment used variations of two established methods to measure wooded vegetation in the field. The first, developed by [Muir et al. \(2011\)](#) as the Australian national guidelines. This method was used to collect 300 point intercepts at one metre intervals along three separate 100 m linear transects arranged in a star pattern of 0°, 60° and 120° orientation. Using a densitometer or vertical sighting tube to record upper wooded canopy cover, generally at a height above 2 m, and a downward pointing laser pointer to record mid and under-storey wooded cover below 2 m high, at each metre intercept location. The second method developed by [White et al. \(2012\)](#) is a further adaptation of the [Muir et al. \(2011\)](#) method. Utilising the same point intercept collection method it differs in that 1000 m spaced intercepts are collected along a grid pattern of 10 individual 100 m linear transects. Both methods are relatively labour intensive with the later requiring a substantially longer period of time to complete. On average the first method requires 1–2 h and the second 4–5 h for two operators to complete in a moderately timbered environment. Both methods are illustrated in [Fig. 4](#). One of the training field sites on OMP of average wooded cover was intensively sampled with the [White et al. \(2012\)](#) method. A further seven independent field sites on a pastoral property to the south of the study area with similar wooded vegetation communities were sampled with the less intensive method of [Muir et al. \(2011\)](#). In both methods alive and dead wooded foliage, stem and branches were recorded across the upper, mid and ground vegetation stratum and combined. Upper Mid Ground Foliage Projected Cover (UMG_{FPC}) was calculated in a similar manner to [Armston et al. \(2009\)](#) and [Staben et al. \(2016\)](#), as the total number of green intercepts divided by the total number of intercepts minus stem occlusions as a percentage of the site covered by green wooded vegetation. Upper Mid Ground Plant Projected Canopy Cover (UMG_{PPC}) was also calculated in the same manner as UMG_{FPC} with the exception that it included both green and dead wooded foliage and branch/stem material. The latter was calculated to account for the often difficult field distinction of live versus dead leaf material in fine leaved arid woody vegetation. The proportion of ortho-mosaic classified wooded cover across the extent of each measured field site was next calculated as a sites average Aerial Photography Wooded Cover (AP_{WC}) and compared with each sites corresponding estimates of both UMG_{PPC} and UMG_{FPC} . Similar statistical methods employed by [Staben et al. \(2016\)](#) to compare wooded cover measurements derived from historical aerial photography with that of associated field data were adapted and applied. An independent students *t*-test was used to assess statistical differences between the field and image estimates of wooded cover. The Pearson's product moment correlation coefficient was employed to determine correlation between modelled and field measured and the root mean square error reported the overall accuracy of each comparison.

3.3.6. Geometric accuracy

A test site was chosen to assess the geometric error in both the ortho-mosaic processing and aircraft GPS/GNSS system. Ground control targets were positioned at each corner and centre point of the chosen site. A Ublox® NEO-M8T differential GPS receiver was used as a rover device to collect ground control target positions and later post processed with the closest (< 30 km) [Geoscience-Australia \(2018\)](#) hourly rinex base-station observations using the open-source RTKLIB software tool kit. The distance from the ground control target identified in the ortho-mosaic image and its differentially corrected position was calculated and reported as the error.

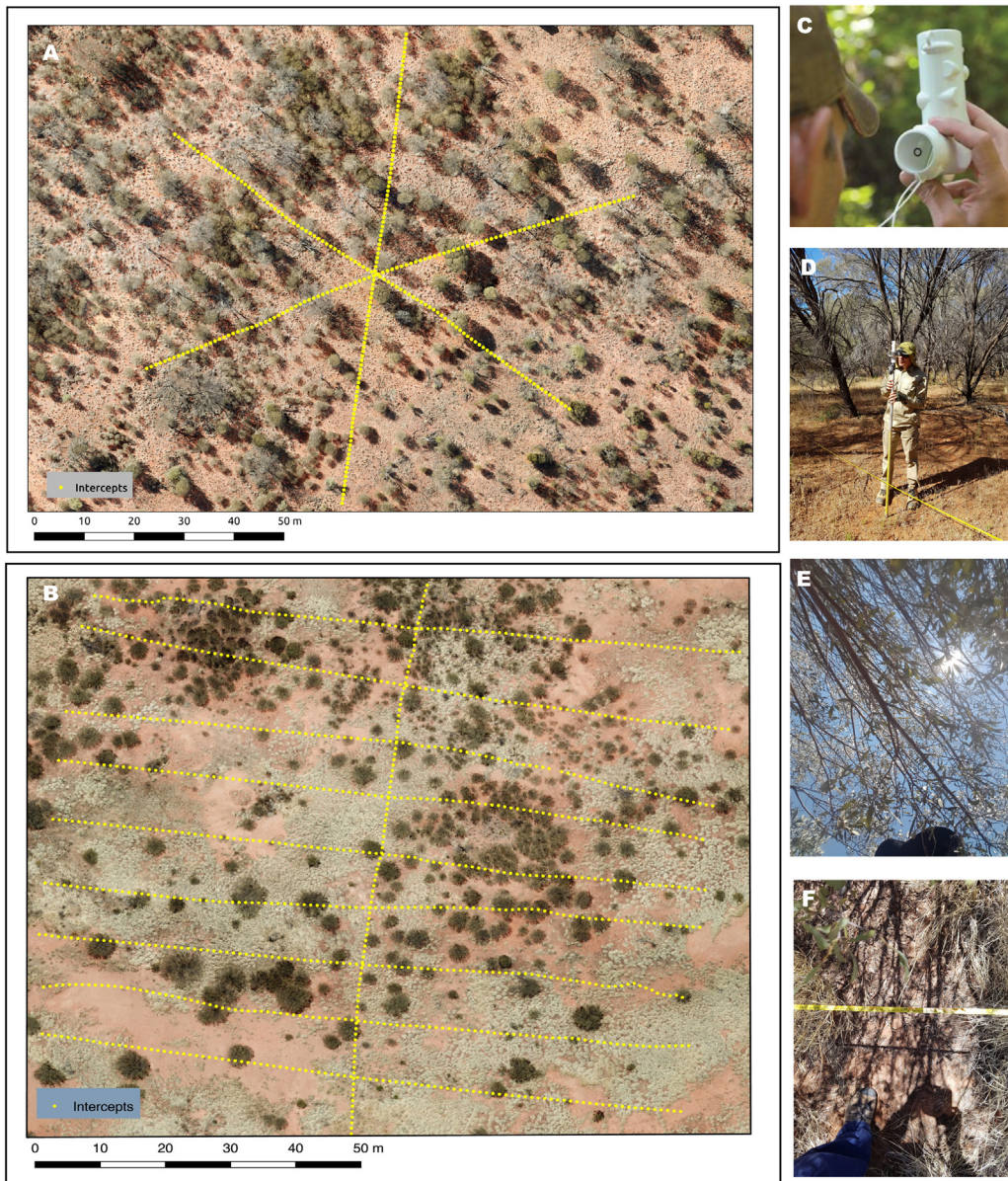


Fig. 4. Wooded cover point intercept field measurements. (A) Star pattern of 300 intercepts, (B) grid pattern of 1000 intercepts, (C) use of densitometer to identify over-storey intercept (B) densitometer and laser pointer intercept collection method, (C) over-storey and under-storey intercept examples.

4. Results

4.1. Wooded cover classification

4.1.1. Satellite image classifications

The random forest classifier was selected by the TPOT optimisation process as the highest performing classifier for each satellite sensor. The optimised input parameters as a result of the process are further detailed in Table 3. Each satellite image classification is shown in Fig. 5 and illustrates the performance of each classification. A subset of the RPAS imagery for an area of densely wooded vegetation (class 3), that was not used to train the classification is also shown to compare the outputs of each classification.

4.1.2. Accuracy assessments

The proportions of each classified cover class including non-wooded cover are detailed in Table 4 and highlight the differences in each classifications assignment of classes. Next the overall classification accuracy's and kappa statistics of each satellite sensor are summarised in

Table 3

Random forest machine-learning model optimised parameter values.

Parameters	Classifiers		
	Lsat8	Sent2	Planet Dove
N. estimators	500	500	500
Criterion	Gini	Gini	Gini
Max. features	0.05	0.15	0.4
Min. split	3	7	4
Min. leaf	1	13	4

each confusion matrix in Table 5. The Planet Dove classification had the highest overall accuracy followed by Sentinel2 and Landsat8. The overall commission and omission errors followed similar trends however the Kappa statistic was slightly better in the Sentinel2 classification than Planet Dove and Landsat8. Each sensor classifications accuracy and error is further illustrated in Fig. 6. The variability of each measure is seen to be lowest in the Planet Dove classification. Next each

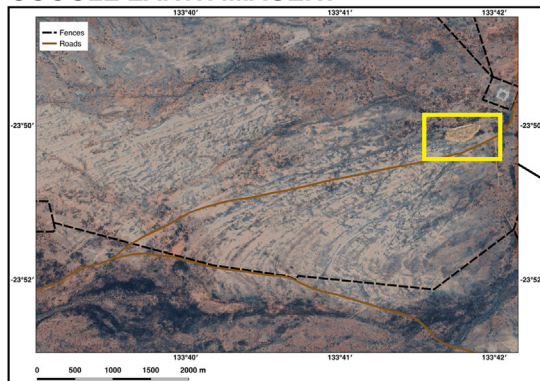
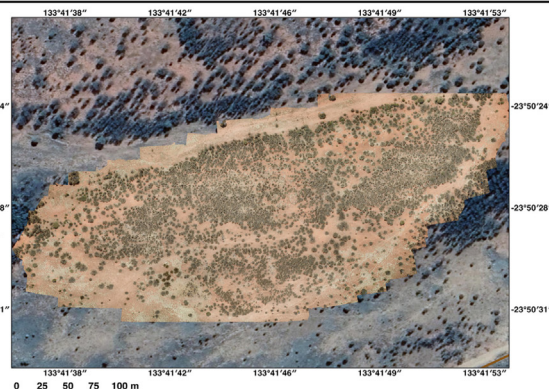
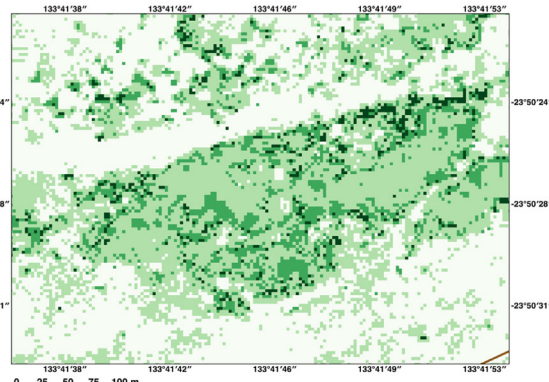
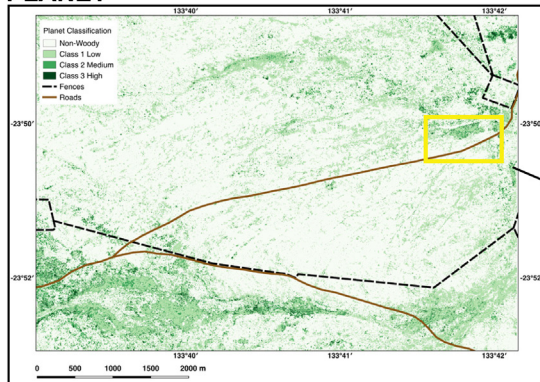
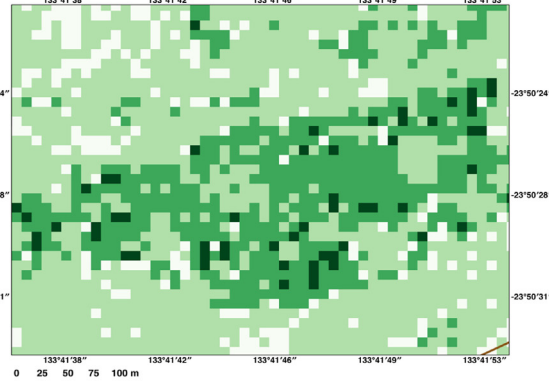
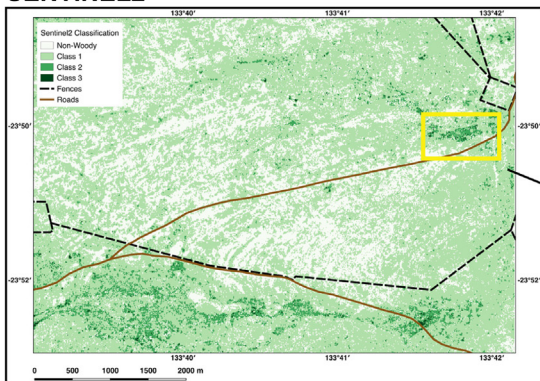
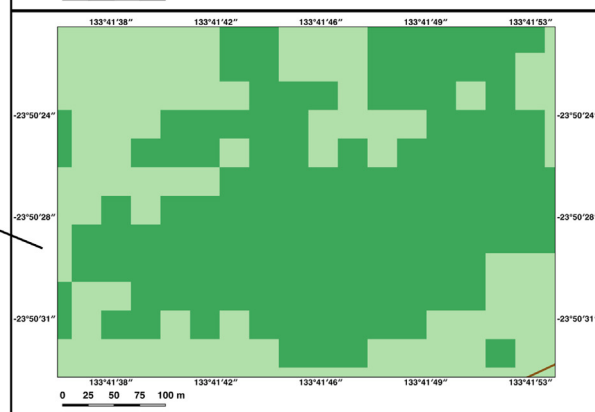
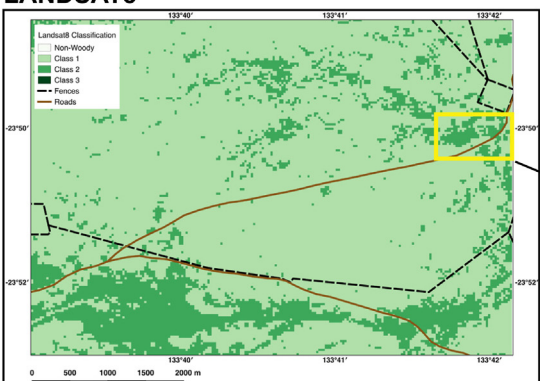
GOOGLE EARTH IMAGERY**INSETS****PLANET****SENTINEL2****LANDSAT8**

Fig. 5. Wooded cover classifications of each satellite image. A subset area of wooded cover is shown to highlight differences in scale and mapped wooded cover.

Table 4
Proportions of classification cover classes.

Class	Classification		
	Lsat8	Sent2	Planet Dove
Non-wooded	0	29	71.4
Class 1 (Low)	81.9	65.7	23.9
Class 2 (Medium)	18.1	5	3.6
Class 3 (High)	0.1	0.3	1.1

Table 5
Confusion matrices and accuracy assessments of each classification.

<i>Planet Dove</i>						
Class	NW	C1	C2	C3	Total	User %
NW	2172	324	4	1	2501	87
C1	689	667	33	7	1396	48
C2	95	209	24	5	333	71
C3	31	86	13	8	138	6
Totals	2987	1286	74	21	2871	—
Producer (%)	73	52	32	38	—	—

Wooded cover class key
NW = non-woody, C1 = class 1 (1–27%), C2 = class 2 (27–53%), C3 = class 3 (53–100%)

<i>Sentinel2</i>						
Class	NW	C1	C2	C3	Total	User %
NW	81	42	0	0	123	66
C1	30	133	8	0	171	78
C2	2	35	16	1	54	30
C3	1	8	10	1	20	5
Totals	114	218	34	2	231	—
Producer (%)	71	61	47	50	—	—

Wooded cover class key
NW = non-woody, C1 = class 1 (1–16%), C2 = class 2 (16–32%), C3 = class 3 (32–100%)

<i>Landsat8</i>						
Class	NW	C1	C2	C3	Totals	User %
NW	0	3	1	0	4	0
C1	1	12	2	0	15	80
C2	0	2	3	1	6	50
C3	0	0	1	2	3	67
Totals	1	17	7	3	17	—
Producer (%)	0	71	43	67	—	—

Wooded cover class key
NW = non-woody, C1 = class 1 (1–8%), C2 = class 2 (8–16%), C3 = class 3 (16–27%)

classification confusion matrix is detailed in Table 5. Producer accuracies are similar for all non-wooded and wooded classes across sensors. The user accuracies however varied between sensors and classes. The Planet Dove non-wooded class was highest overall and the Sentinel2 wooded classes were in comparison significantly higher for wooded classes one and two.

4.2. Wooded cover sampling

4.2.1. Field data validation

The result of the comparison of AP_{WC} with that of both UMG_{PPC} and UMG_{FPC} for the seven field sites, six collected utilising the (Muir et al., 2011) method and one with the method of White et al. (2012), are detailed in Table 6. The result of the comparison show an overall strong relationship between AP_{WC} with that of both UMG_{PPC} and UMG_{FPC}, with UMG_{FPC} showing the strongest relationship. Fig. 7 further illustrates the relationships between field measured UMG_{PPC}/UMG_{FPC} and AP_{WC} for both methods of collection. The result of the independent t-test ($\alpha = 0.01$) show that neither UMG_{PPC} or UMG_{FPC} are significantly different to that of the mean values of AP_{WC}.

4.2.2. RPAS ortho-mosaic geometric accuracy

An assessment of the geometric error of the combined ortho-mosaic processing and RPAS GPS accuracy resulted in an average displacement of 2.4 m. The Ground Control Point (GCP) displacement measurement of the five GCP targets from their associated differential GPS location is shown in Table 7.

5. Discussion

Knowledge of the extent and change in wooded vegetation across the arid rangelands of Australia is limited. Due in part to access to large area high resolution satellite imagery and appropriate field based methods to adequately and efficiently sample wooded arid vegetation. This study investigated the development of a wooded vegetation classification using recent developments in the availability of high resolution, large area satellite imagery, and the use of a low cost RPAS to more efficiently and accurately sample wooded vegetation.

First the RPAS derived aerial photography classification was assessed for both its ability to produce a high resolution ortho-mosaic image with an acceptable level of geometric precision. Further object based segmentation and classification, provided an estimation of the extent of wooded vegetation cover over a series of field sites comparable to that of two accepted field based measures of wooded cover. The geometric error assessment of a field site showed an average displacement of 2.4 m. The potential misalignment with the satellite imagery varies between sensors. The effect upon the classification accuracy is difficult to predict and should form the basis of further work. Resource limitations prevented this study in carrying out further differential GPS collection.

Next, the comparison of AP_{WC} with that of both UMG_{PPC} and UMG_{FPC} indicate a strong relationship between the RPAS derived aerial photography classification and field measured wooded cover. The correlation measures in Table 6 indicate that UMG_{FPC} was the strongest of the two field based measurements. Fig. 7 illustrates an overestimation in AP_{WC} for the UMG_{FPC} field parameter. This is not as evident in the UMG_{PPC} comparison. Over and under estimation is evident in both the field based method of measuring wooded cover and the RPAS derived aerial photography classification, making it difficult to determine the degree of error in each method. The intensive method of White et al. (2012) is both under and over-estimated in both instances, indicated by the red points in Fig. 7, and suggests that improvements to the RPAS derived aerial photography classification method is needed. Improvements to the segmentation process of the classification method could improve the accuracy through better separation of wooded and non-wooded vegetation as well as the use of higher resolution imaging with a more sophisticated RPAS sensor. However the result of the independent t-test indicates that differences between field measured wooded cover and the RPAS derived aerial photography classification were not statistically significant and it can be concluded that the study was successful in developing a comparative method to that of the point intercept method of Muir et al. (2011) and White et al. (2012) to accurately sample wooded cover in arid sparse vegetation in a repeatable

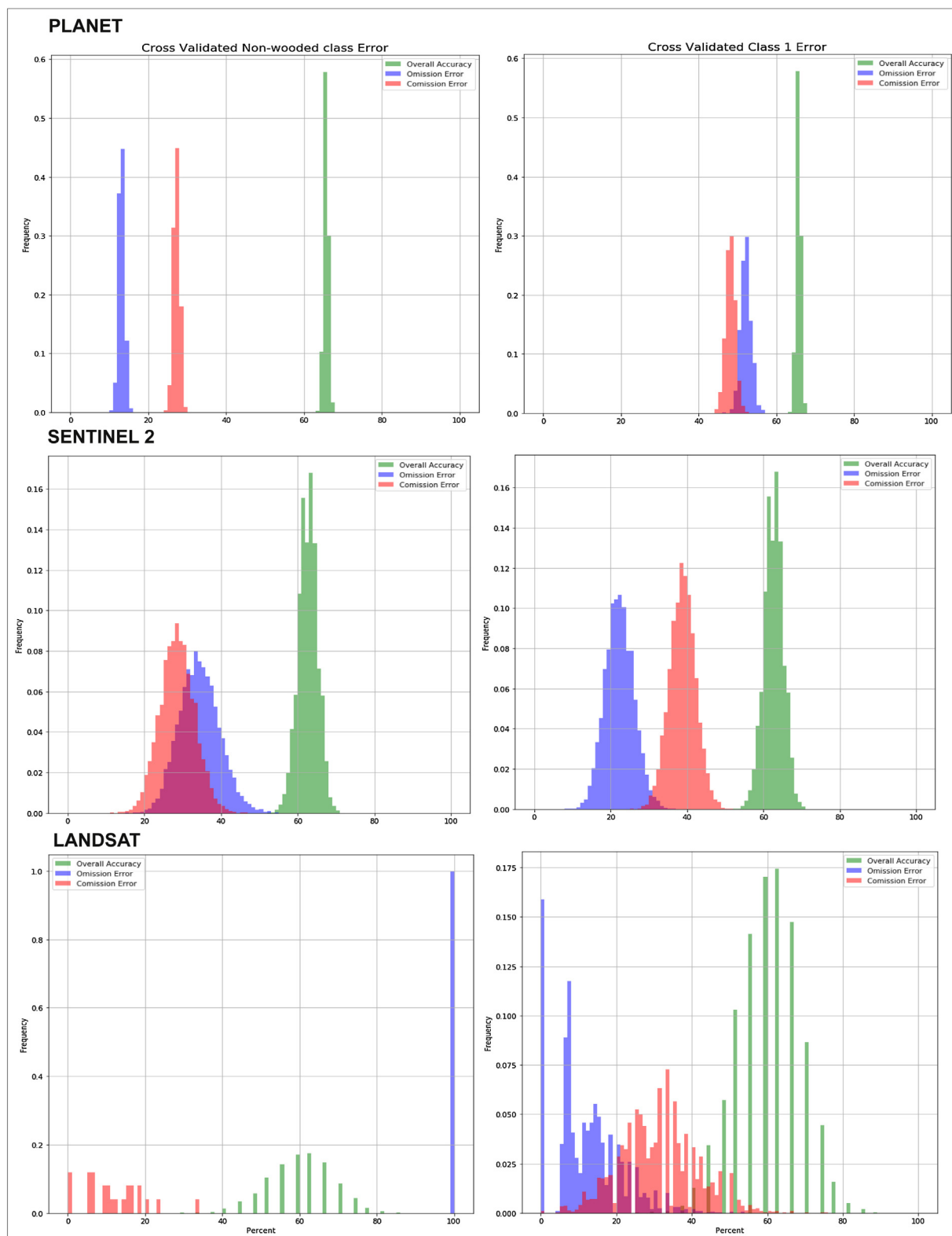


Fig. 6. Output plots of accuracy simulation results for each wooded cover class by satellite sensor. The frequency distribution of each classes overall accuracy is presented in green, omission error in blue and commission error in red. (For interpretation of the references to colour in this figure legend, the reader is referred to the web version of this article.)

and resource efficient manner.

The Sentinel2 and Planet Dove classification results are compared to that of the Landsat8 classification. The Sentinel2 and Planet Dove overall classification accuracy's were marginally higher at 65.7% and 62.7% compared to that of 62.1% for Landsat8. The kappa statistics

were also very similar between classifications with the Sentinel2 classification the highest at 0.38 then Landsat8 at 0.35 and interestingly Planet Dove the lowest at 0.33, although these differences are only very marginal and likely not significant. The kappa statistic demonstrates the overall medium to low level of classification accuracy. The individual

Table 6

Comparison of RPAS derived wooded cover with that of field measured wooded cover parameters.

Wooded parameter	<i>r</i>	RMSE	<i>T</i> statistic	<i>P</i> value
UMG _{FPC}	0.96	5.14	1.35	0.20
UMG _{PPC}	0.88	3.67	0.11	0.91

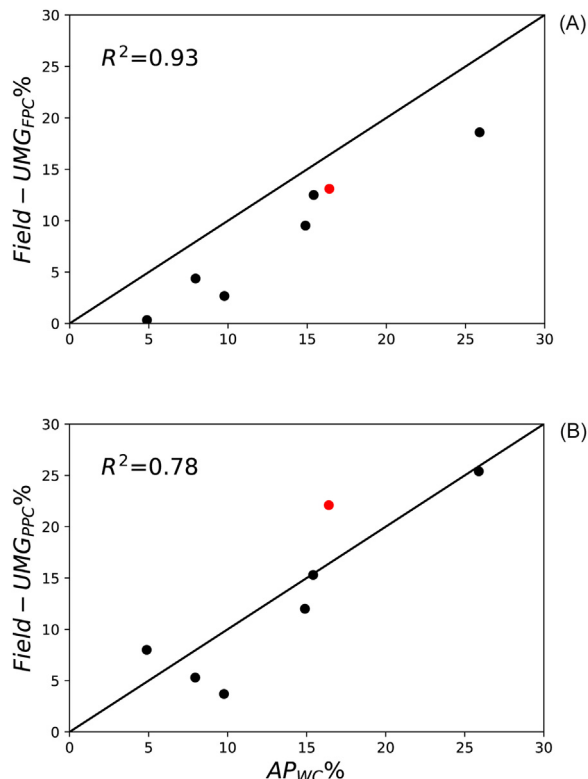


Fig. 7. Scatter plot illustrating the relationships between field measures wooded cover and the RPAS classification of wooded cover. Plot (A) is the comparison of AP_{WC} with that of field UMG_{FPC} and plot (B) a comparison of AP_{WC} with field UMG_{PPC}. The black points in both plots indicate those sites collected with the star transect method and the single red point the site collected with the more intensive grid pattern method. (For interpretation of the references to colour in this figure legend, the reader is referred to the web version of this article.)

Table 7

RPAS ortho-mosaic ground control point displacements (mm).

Top left	Top right	Bottom right	Bottom left	Centre
2801	2470	2282	1765	2810

class user accuracy's provide greater detail of the differences between classifications. The non-wooded (NW) class for Landsat8 scored zero with no correct user or producer classifications for this class. The low number of training pixels for this class, only 16% of the training dataset, suggests more training sites were needed, however the coarser scale of the imagery and its effect upon the mixture of low wooded and non-wooded cover is a contributing factor to the classification. The highest overall omission error for the Landsat8 classification at 54% reflects this classification. The NW and C1 (Low-cover) classes of both the Sentinel2 and Planet Dove classifications are markedly different. Sentinel2 NW is 87% and Planet Dove 66%, and C1 is 77% and 48% respectively. The Planet Dove classification performed better in distinguishing between NW and C1 compared to that of Sentinel2 and

Landsat8. However, Sentinel2 and Landsat8 both demonstrate a higher user accuracies in all the wooded classes. The higher spatial resolution of the Planet Dove imagery is a likely contributing factor to its improved accuracy in classifying non-wooded cover as well as distinguishing the sparsely spaced canopies or clumps of both wooded cover species. The higher radiometric resolution of the Sentinel2 and to a degree Landsat8 imagery is also a likely explanation for the improved performance in the wooded classes in comparison to the Planet Dove classification.

The mapped classifications of each sensor are presented in Fig. 5 as both the overall extent of each classification and a subset of an area of wooded cover not used in the training of the classification. Differences in the spatial scale of each classification are apparent. Both the Planet Dove and Sentinel2 subsets define the extent of the wooded cover as well as the patterns of both wooded and non-wooded cover within its extent whereas the Landsat subset provides just an overall extent. Differences in the degree of wooded cover is most apparent in the Planet Dove subset and field investigations of the subset area confirmed differences in wooded cover species. The higher class of wooded cover related to *A. kempeana* (Witchetty Bush) species and the low to medium class that of *A. aneura* (Mulga). Fig. 2 illustrates differences in the leaf structures of both species. Mulga has thinner needle like leaf adaptations whereas Witchetty Bush has broader and greener leaves or phyllodes. Differences in the degree of detectable green leaf matter between these two dominant wooded vegetation species are the likely contributing factors to the observable differences in classified wooded vegetation cover for the Planet Dove classification and to a lesser degree Sentinel2. Mixtures of wooded and non-wooded cover is apparent in both the classifications and observed on the ground. The Planet Dove classification had the least degree of mixing in the lower cover class, Sentinel2 was affected to some degree and Landsat8 the most.

Fig. 6 illustrates the degree and variability of each classifications overall accuracy and their associated cover classes omission and commission error. This provides further insights into the performance of each classification and the differences between them. The model sensitivity to training data is least in Planet Dove and greatest in the Landsat8 classifications. The degree and variability of omission and commission error varies between classes and classifications. In both the Planet Dove and Sentinel2 classifications both errors gradually increase from the non-wooded class to the medium wooded class, whereas the Landsat8 classification of non-wooded cover exhibits the highest proportion of omission error. The spatial and radiometric resolution differences between each sensor and their classifications are contributing factors as previously discussed.

6. Conclusions and further research

This study demonstrated that higher spatial resolution satellite imagery improves the classification of wooded vegetation cover in the arid rangelands of Australia, in particular the separation of low wooded vegetation cover from non-wooded cover. This exposes the limits of Landsat imagery for monitoring slow woody cover change in arid woodlands. This is evident when woody change is the result of thickening and thinning rather than invasion into a grassland. Improvements to classification methods including the use of machine learning methods, in particular optimisation methods to select the most appropriate algorithms and input parameters, contributed to an improved mapping result. The large amount of training data required to inform a machine learning method is a limitation. This is particularly apparent with coarse scale imagery such as Landsat. This study however proved that a more efficient method of collecting field training data is possible with the use of a RPAS. Further studies should both aim to improve the RPAS segmentation method and explore the use of more sophisticated RPAS image sensing. In particular the use of multi-spectral sensing in both the near and short wave infra-red spectrum as a useful tool to separate wooded from non-wooded vegetation in low-photosynthetic

overall vegetation. In addition further research should focus on the use of photogrammetry methods to distinguish structure from motion to further inform the separation of wooded from non-wooded based on the height profile of the vegetation. The presence and degree of cast shadow and its effect upon the accuracy of future wooded cover classifications should also be further investigated, to determine the need for optimal seasonal and daily acquisition time-frames for both satellite and RPAS borne imagery.

The spectral un-mixing approach of Wang et al. (2015) demonstrated a method of deriving wooded vegetation cover from Landsat imagery that varied in accuracy with the presence/absence of non-woody herbaceous vegetation as a function of climate response, the effects this would have upon the methods used in this study remain unknown and should form the basis of further research involving the collection of RPAS imagery and classification of wooded cover from high spatial resolution imagery across a range of non-woody herbaceous vegetation growth stages. The use of spectral un-mixing methods with high spatial resolution sensors such as the ones used in this study is limited by the absence of further spectral bands at the same spatial resolution, particularly the short wave infra-red band and its benefits already discussed. This study has shown that the suggestions offered by Gill et al. (2017) and Fisher et al. (2016) around improved classification with high resolution imagery in arid environments are indeed true.

Authors' contribution

Prof. Stuart Phinn and Dr. Peter Scarth provided support, advice and supervision as Ph.D. advisors of the primary author. Jason Barnettson conducted the research and wrote the paper.

Acknowledgements

Support from the Australian Government Research Training Program Scholarship. Support and funding from the University of Queensland Joint Remote Sensing Research Agreement. Support and funding from the NT Department of Environment and Natural Resources/QLD Department of Science, Information Technology and Innovation Collaborative Research Agreement. QLD Department of Science, Information technology and Innovation staff at the Eco-sciences Precinct Remote Sensing Centre for assistance, support, training, advice and access to High Performance Computing Infrastructure. NT Department of Environment and Natural Resources staff and volunteers for assistance in collecting field data including Andrew Scott and Cameron Wallace.

References

- ABARES, 2016. The Australian Land Use and Management Classification Version 8. Tech. Rep. Australian Bureau of Agricultural and Resource Economics and Sciences, Canberra, ACT. http://www.agriculture.gov.au/abares/documents/ALUMCv8_Handbook4ednPart2_UpdateOctober2016.pdf.
- Armston, J.D., Denham, R.J., Danaher, T.J., Scarth, P.F., Moffiet, T.N., 2009. Prediction and validation of foliage projective cover from Landsat-5 TM and Landsat-7 ETM+ imagery. *J. Appl. Rem. Sens.* 3 (1), 33528–33540. <https://doi.org/10.1117/1.3216031>.
- Bowman, D., Boggs, G.S., Prior, L.D., 2008. Fire maintains an *Acacia aneura* shrubland – Triodia grassland mosaic in central Australia. *J. Arid Environ.* 72 (1), 34–47. <https://doi.org/10.1016/j.jaridenv.2007.04.001>.
- Cohen, J., 1960. A coefficient of agreement for nominal scales. *Educ. Psychol. Meas.* 20 (1), 37–46. <https://doi.org/10.1177/001316446002000104>.
- Danaher, T., Scarth, P., Armston, J., Collett, L., Kitchen, J., Gillingham, S., 2010. Remote sensing of tree-grass systems: the eastern Australian woodlands. pp. 175–194. <https://doi.org/10.1201/b10275>.
- DENR, 2017. Northern Territory Pastoral Land Board Annual Report 2016–2017. Tech. Rep. Northern Territory Department of Environment and Natural Resources, Darwin, Northern Territory. https://denr.nt.gov.au/_data/assets/pdf_file/0006/540573/Pastoral-Land-Board_AR-2016-17_LR.pdf.
- Fensham, R.J., 2008. A protocol for assessing applications to selectively clear vegetation in Australia. *Land Use Policy* 25 (2), 249–258. <https://doi.org/10.1016/j.landusepol.2007.07.001>.
- Fisher, A., Danaher, T., Gill, T., 2017. Mapping trees in high resolution imagery across large areas using locally variable thresholds guided by medium resolution tree maps. *Int. J. Appl. Earth Observ. Geoinform.* 58, 86–96. <https://doi.org/10.1016/j.jag.2017.02.004>.
- Fisher, A., Day, M., Gill, T., Roff, A., Danaher, T., Flood, N., 2016. Large-area, high-resolution tree cover mapping with multi-temporal spot5 imagery, New South Wales, Australia. *Rem. Sens.* 8 (6). <https://doi.org/10.3390/rs8060515>.
- Flood, N., 2014. Continuity of reflectance data between Landsat-7 ETM+ and Landsat-8 OLI, for both top-of-atmosphere and surface reflectance: a study in the Australian landscape. *Rem. Sens.* 6 (9), 7952–7970. <https://doi.org/10.3390/rs6097952>.
- Flood, N., 2017. Comparing Sentinel-2A and Landsat 7 and 8 using surface reflectance over Australia. *Rem. Sens.* 9 (7). <https://doi.org/10.3390/rs9070659>.
- Flood, N., Danaher, T., Gill, T., Gillingham, S., 2013. An operational scheme for deriving standardised surface reflectance from Landsat TM/ETM+ and SPOT HRG imagery for Eastern Australia. *Rem. Sens.* 5, 83–109. <https://doi.org/10.3390/rs5010083>.
- Gardiner, D., Tupper, G., Dundeon, G., 1998. A quantitative appraisal of woody shrub encroachment in western New South Wales. *Rangeland J.* 20 (1), 26–40.
- Geoscience-Australia, 2018. Continuously Operating Reference Stations. <http://auscors.ga.gov.au/status/>.
- Gill, T., Johansen, K., Phinn, S., Trevithick, R., Scarth, P., Armston, J., 2017. A method for mapping Australian woody vegetation cover by linking continental-scale field data and long-term Landsat time series. *Int. J. Rem. Sens.* 38, 679–705. <https://doi.org/10.1080/01431161.2016.1266112>.
- Gill, T.K., Phinn, S.R., Armston, J.D., Paulthorpe, B.A., 2009. Estimating tree-cover change in Australia: challenges of using the MODIS vegetation index product. *Int. J. Rem. Sens.* 30, 1547–1565. <https://doi.org/10.1080/01431160802509066>.
- Jenks, G., 1967. The data model concept in statistical mapping. *Int. Yearb. Cartogr.* 7, 186–189.
- Lawrence, R., Bunn, A., Powell, S., Zambon, M., 2004. Classification of remotely sensed imagery using stochastic gradient boosting as a refinement of classification tree analysis. *Rem. Sens. Environ.* 90 (3), 331–336. <https://doi.org/10.1016/j.rse.2004.01.007>.
- Lennartz, R., Whitehouse, D., 2002. Land Resources of the Eastern Portion of Owen Springs Station. Tech. Rep. Northern Territory Department of Infrastructure, Planning and Environment, Alice Springs, NT. http://www.territorystories.nt.gov.au/jspui/bitstream/10070/238842/1/Land_Resources_of_the_Eastern_Portion_of_Owen_Springs_Station.pdf.
- Lu, H., Raupach, M.R., McVicar, T.R., Barrett, D.J., 2003. Decomposition of vegetation cover into woody and herbaceous components using AVHRR NDVI time series. *Rem. Sens. Environ.* 86 (1), 1–18. [https://doi.org/10.1016/S0034-4257\(03\)00054-3](https://doi.org/10.1016/S0034-4257(03)00054-3).
- Ludwig, J.A., Bastin, G., Wallace, J.F., McVicar, T.R., 2006. Assessing landscape health by scaling with remote sensing: when is it not enough? *Landsc. Ecol.* 22 (2), 163–169. <https://doi.org/10.1007/s10980-006-9038-6>.
- Lyons, M.B., Keith, D.A., Phinn, S.R., Mason, T.J., Elith, J., 2018. A comparison of resampling methods for remote sensing classification and accuracy assessment. *Rem. Sens. Environ.* 208, 145–153. <https://doi.org/10.1016/j.rse.2018.02.026>.
- Muir, J., Schmidt, M., Tindall, D., Trevithick, R., Scarth, P., Stewart, J., 2011. Field Measurement of Fractional Ground Cover: A Technical Handbook Supporting Ground Cover Monitoring for Australia. Tech. Rep. prepared by the Queensland Department of Environment and Resource Management for the Australian Bureau of Agricultural and Resource Economics and Sciences, Canberra. https://www.researchgate.net/publication/236022381/Field_measurement_of_fractional_ground_cover.
- National Land and Water Resources Audit, 2001. Rangelands – Tracking Changes: Australian Collaborative Rangeland Information System. Tech. Rep. National Land and Water Resources Audit, Canberra, ACT. http://www.environment.gov.au/land_rangelands/acris.
- Noble, J.C., 1998. The Delicate and Noxious Scrub: CSIRO Studies on Native Tree and Shrub Proliferation in the Semi-Arid Woodlands of Eastern Australia. CSIRO Publishing, Victoria. <https://doi.org/10.1071/RJ9990260>.
- Olson, R.S., Urbanowicz, R.J., Andrews, P.C., Lavender, N.A., Kidd, L.C., Moore, J.H., 2016. Automating biomedical data science through tree-based pipeline optimization. In: Squillero, G., Burelli, P. (Eds.), Applications of Evolutionary Computation. Springer International Publishing, Cham, pp. 123–137. https://doi.org/10.1007/978-3-319-31204-0_9.
- Peel, M.C., Finlayson, B.L., McMahon, T.A., 2007. Updated world map of the Köppen–Geiger climate classification. *Hydrol. Earth Syst. Sci. Discuss.* 4 (2), 439–473. <https://doi.org/10.5194/hessd-4-439-2007>.
- PlanetLabs, 2016. Planet Imagery Product Specification: Planetscope & Rapideye. Tech. Rep. <https://www.planet.com/products/satellite-imagery/files/1610.06/SpecSheet/Combined/Imagery/Product/Letter/ENGv1.pdf>.
- PlanetLabs, 2018. Surface Reflectance Technical White Paper. Tech. Rep. https://assets.planet.com/marketing/PDF/Planet_Surface_Reflectance_Technical_White_Paper.pdf.
- Rodriguez-Galiano, V., Ghimire, B., Rogan, J., Chica-Olmo, M., Rigol-Sánchez, J., 2012. An assessment of the effectiveness of a random forest classifier for land-cover classification. *ISPRS J. Photogram. Rem. Sens.* 67, 93–104. <https://doi.org/10.1016/j.isprsjprs.2011.11.002>.
- Sculley, D., 2010. Web-scale k-means clustering. Proceedings of the 19th International Conference on World Wide Web, WWW10. ACM, New York, NY, USA, pp. 1177–1178. <https://doi.org/10.1145/1772690.1772862>.
- Sinclair, R., 2005. Long-term changes in vegetation, gradual and episodic, on the TGB Osborn Vegetation Reserve, Koonamore, South Australia (1926–2002). *Austr. J. Bot.* 53 (4), 283–296. <http://search.proquest.com/docview/20281694/>.
- Staben, G., Lucieer, A., Evans, K., Scarth, P., Cook, G., 2016. Obtaining biophysical measurements of woody vegetation from high resolution digital aerial photography in tropical and arid environments: Northern Territory, Australia. *Int. J. Appl. Earth Observ. Geoinform.* 52, 204–220. <https://doi.org/10.1016/j.jag.2016.06.011>.
- Vedaldi, A., Soatto, S., 2008. Quick shift and kernel methods for mode seeking. In:

- Forsyth, D., Torr, P., Zisserman, A. (Eds.), Computer Vision – ECCV 2008. Springer, Berlin, Heidelberg, pp. 705–718. <https://doi.org/10.1007/978-3-540-88693-8-52>.
- Wang, K., Franklin, S.E., Guo, X., Cattet, M., 2010. Review from the perspective of remote sensing specialists. *Sensor (Basel)* (11), 9647–9667. <https://doi.org/10.3390/s101109647>.
- Wang, Z., Bastin, G., Liu, L., Caccetta, P., Peng, D., 2015. Estimating woody above-ground biomass in an arid zone of central Australia using Landsat imagery. *J. Appl. Rem. Sens.* 9. <https://doi.org/10.1111/jrs.9.096036>.
- White, A., Sparrow, B., Leitch, E., Foulkes, J., Flitton, R., Lowe, A., Caddy-Retalic, S., 2012. AusPlots Rangelands Survey Protocols Manual. Tech. Rep. Terrestrial Ecosystem Research Network, Adelaide. <https://www.tern.org.au/AusPlots-Rangelands-Survey-Protocols-Manual-pg23944.html>.
- Witt, G., Harrington, R., Page, M., 2009. Is ‘vegetation thickening’ occurring in Queensland’s mulga lands – a 50-year aerial photographic analysis. *Austr. J. Bot.* 57 (7), 572–582. <https://doi.org/10.1071/BT08217>.
- Zandler, H., Brenning, A., Samimi, C., 2015. Quantifying dwarf shrub biomass in an arid environment: comparing empirical methods in a high dimensional setting. *Rem. Sens. Environ.* 158, 140–155. <https://doi.org/10.1016/j.rse.2014.11.007>.